Collisionless damping of parametrically unstable Alfvén waves

J. A. Araneda,[1] E. Marsch,[2] and A. F. Viñas[3]

Received 1 August 2006; revised 31 October 2006; accepted 29 November 2006; published 28 April 2007.

[1] Linear Vlasov theory and one-dimensional hybrid simulations are used to study the parametric instabilities of a circularly polarized parallel propagating Alfvén wave in a homogeneous, magnetized, and collisionless plasma. We discuss the linear and the weakly nonlinear development of the instabilities of the Alfvén waves, including kinetic effects, and investigate the structure, the growth, and the damping of the driven ion acoustic-like waves. The dispersion relation reproduces the fluid characteristics of the instabilities in the case that protons are cold but contains an infinite number of roots in the general case. We show that at low proton plasma β_p ($\beta_p \approx 0.1$), kinetic effects break the degeneracy of the mode-coupling solutions of the fluid theory, and we unambiguously identify the growing and the damped modes. We find that contrary to traditional thought, kinetic effects are important even for very low-β_p in the late stages of the linear evolution, leading to a dephasing effect between the plasma pressure and the density fluctuations. The relevance of the results to the experimental identification of the instabilities, to the generation of local turbulence, and to the reduction of cross helicity in the solar wind are pointed out.

Citation: Araneda, J. A., E. Marsch, and A. F. Viñas (2007), Collisionless damping of parametrically unstable Alfvén waves, *J. Geophys. Res.*, *112*, A04104, doi:10.1029/2006JA011999.

1. Introduction

[2] The nonlinear stability of finite-amplitude circularly polarized Alfvén waves propagating along a background magnetic field has been a matter of continuous research in the last 30 years [e.g., *Derby*, 1978; *Goldstein*, 1978; *Longtin and Sonnerup*, 1986; *Wong and Goldstein*, 1986; *Brodin and Stenflo*, 1988; *Viñas and Goldstein*, 1991a, 1991b; *Ghosh et al.*, 1993; *Hollweg*, 1994; *Ruderman and Simpson*, 2004]. The interest in this subject is based on a remarkable property of Alfvén waves, namely that they are nonlinear eigenmodes of the magnetohydrodynamic (MHD) equations. These waves have also received much attention in the plasma literature because they occur ubiquitously in space plasmas *Belcher and Davis* [1971] and the interstellar medium *Minter and Spangler* [1997]. They are believed to play an important role in coronal heating, solar wind acceleration and the development of the turbulent structure of the solar wind plasma [e.g., *Tu and Marsch*, 1995, 2001; *Bruno and Carbone*, 2005; *Wang et al.*, 2006]. However, finite-amplitude Alfvén waves are unstable to parametric decay in which the energy of the parent wave is gradually transferred to compressible acoustic-like waves and other fluctuations. Since compressive fluctuations can be damped through kinetic effects, an understanding of the relationship between Alfvén wave activity and density fluctuations is of great interest, not only in basic plasma physics but also in application to space and astrophysical plasmas.

[3] A two-fluid analysis of the stability of a circularly polarized Alfvén (pump) wave propagating with wave number k_0 parallel to a mean field $\mathbf{B}_0$ shows that the pump wave is unstable to the growth of several parametric instabilities. The excitation of a compressional (acoustic-like) daughter wave with $k < k_0$ generates a modulational instability. The modulation wave is characterized by a longer wavelength than that of the pump wave. This instability occurs only in the presence of ion wave dispersion and usually involves an interaction of two forward propagating Alfvén waves with wave numbers $k_0 - k$ and $k_0 + k$ (lower and upper sidebands, respectively). Another instability that also arises for $k < k_0$ but does not extend down to $k = 0$ was found by *Hollweg* [1994]. It is due to an interaction between a forward propagating lower sideband ($-f$) and a forward propagating acoustic-like ($+s$) wave. Two more parametric processes are known to occur, the beat and decay instabilities, which involve density fluctuations with $k > k_0$. The beat instability arises from the interaction of a forward propagating upper sideband ($+f$) and a backward propagating lower sideband ($-b$) wave. An analogous nonlinear coupling occurs also for two high-frequency electromagnetic waves and electron-plasma waves [*Forslund et al.*, 1972]. The decay instability involves the interaction between a $+s$ and $-b$ wave.

[4] Modulational instabilities and Alfvén solitons have been studied, using the derivative nonlinear Schrödinger (DNLS) equation in the work of *Mjølhus* [1976], *Mio et al.* [1976], and *Spangler and Sheerin* [1982]. Fluid theory

[1]Departamento de Física, Facultad de Ciencias Físicas y Matemáticas, Universidad de Concepción, Concepción, Chile.
[2]Max-Planck-Institut für Sonnensystemforschung, Katlenburg-Lindau, Germany.
[3]Laboratory for Solar and Space Physics, NASA Goddard Space Flight Center, Greenbelt, Maryland, USA.

Copyright 2007 by the American Geophysical Union.
0148-0227/07/2006JA011999

predicts a very strong dependence of the instability behavior on β, and on the pump polarization. However, it is known that kinetic effects modify the DNLS equation and produce a modulational instability independent of the plasma β and the polarization mode [*Mjølhus and Wyller*, 1988; *Spangler*, 1989]. Furthermore, numerical solutions of the kinetically modified DNLS equation show that the combined effects of both wave nonlinearity and Landau damping result in the formation of stationary *S*- and *arc*-polarized discontinuities as observed in the solar wind plasma [*Medvedev et al.*, 1997].

[5] On the other hand, *Inhester* [1990], using the drift-kinetic theory, showed that collisionless damping can significantly reduce the growth rate of the decay instability and enlarge the range of wave number over which the instability exists. This result emphasizes the need for a fully kinetic treatment of the problem. For $\beta < 1$, *Terasawa et al.* [1986], using a hybrid code, also found a reduction of the growth rates. However, the decrease was only slight when compared with the rates predicted by fluid theory, while *Vasquez* [1995] also using hybrid simulations, showed that even for moderate amplitude ($\delta B/B_0 < 1/2$) their wave trains produce instabilities and saturated states, which differ completely from the fluid theory results if $\beta > 1$.

[6] Although there has been much progress in characterizing the instabilities of parallel propagating Alfvén waves, a better understanding of the linear and nonlinear kinetic behavior is clearly needed. Furthermore, since the drift-kinetic approach is limited to the case of a large wavelength of the pump wave and neglects dispersion, it prevents the study of the beat and modulational instabilities. On the other hand, the kinetic DNLS equation excludes the decay instability.

[7] The aim of this paper is to carry out a systematic study of both the linear and weakly nonlinear regime of parametric instabilities of parallel propagating Alfvén waves in an electron-proton plasma, including the effects of collisionless damping, and to investigate the structure and the growth and damping rate of the modes caused by the coupling of the pump wave to the plasma.

[8] We propose to use a relatively simple method to incorporate Landau damping into the fluid equations [*Araneda*, 1998]. Instead of closing the fluid moment equations by a polytropic closure equation (or by using a fluid model for Landau damping), we determine the pressure-density relation by a fully kinetic treatment of the ion-acoustic-like wave dispersion relation, thus avoiding the inadequacies of fluid models to describe resonant effects. The outline of this paper is as follows. In section 2, the physics of the model is presented and the dispersion relation which includes Landau damping is derived. In section 3 we carry out an analysis of the parametric instabilities. Computer simulations supporting the analytical results of section 3 are presented in section 4. A summary of the paper and conclusions are given in section 5.

2. Basic Model and Dispersion Relation

[9] The present analysis assumes that a finite-amplitude circularly polarized Alfvén parent (pump) wave propagates along the background magnetic field $\mathbf{B}_0$ in a quasi-neutral electron-proton plasma. We restrict ourselves to low-frequency (far below the electron cyclotron frequency) electromagnetic fluctuations propagating parallel to a constant magnetic field $B_0\hat{\mathbf{z}}$ in the $+z$ direction, and adopt a massless fluid-electron model. Furthermore, because the purpose here is to study the effects of Landau damping on the stability of Alfvén wave trains, we neglect heating in the perpendicular direction. *Vasquez* [1995] has already shown from hybrid simulations that the ion temperatures change very slowly during the linear stage of the instabilities. Therefore we assume that the distribution function (here n_0 is the background density) of the proton component can be represented by

$$F(z, \mathbf{v}, t) = n_0 \delta(\mathbf{v}_\perp - \mathbf{V}_\perp) f(z, v_z, t) \ , \tag{1}$$

whereas the transverse bulk motion of protons is governed by

$$n_e m_p \frac{d\mathbf{V}_\perp}{dt} = n_e e \mathbf{E}_\perp + \left(\mathbf{J}_p \times \mathbf{B}\right)_\perp \ , \tag{2}$$

and quasi-neutrality, $n_e = n_p$ is assumed. In this hybrid kinetic-fluid model, the ion distribution function $F(z, \mathbf{v}, t)$ evolves according to the Vlasov equation:

$$\left[\frac{\partial}{\partial t} + v_z \frac{\partial}{\partial z} + (\mathbf{E} + \mathbf{v} \times \mathbf{B}) \cdot \frac{\partial}{\partial \mathbf{v}}\right] F(z, \mathbf{v}, t) = 0 \ . \tag{3}$$

The electric and magnetic field, $\mathbf{E}(z, t)$ and $\mathbf{B}(z, t)$, are determined self-consistently from Maxwell's equations,

$$\nabla \times \mathbf{E} = -\frac{\partial \mathbf{B}}{\partial t} \ , \tag{4}$$

$$\nabla \times \mathbf{B} = \mu_0 \mathbf{J} \ , \tag{5}$$

where the total current density is

$$\mathbf{J} = \mathbf{J}_e + \mathbf{J}_p \ . \tag{6}$$

The set of equations is completed by the inclusion of the fluid equation for the warm massless electrons,

$$\mathbf{0} = -n_e e \mathbf{E} + \mathbf{J}_e \times \mathbf{B} - \nabla P_e \ . \tag{7}$$

We have neglected the electron inertia force in equation (7), which is equivalent to assuming that the wave frequencies of interest are much less than the electron cyclotron frequency. We have also neglected the displacement current in equation (5). By eliminating the electron variables from equations (5), (6), and (7), we obtain an expression (generalized Ohm's law in the so called Hall-MHD) for the electric field,

$$\mathbf{E} = -\frac{\mathbf{J}_p \times \mathbf{B}}{n_p e} + \frac{(\nabla \times \mathbf{B}) \times \mathbf{B}}{\mu_0 n_p e} - \frac{\nabla p_e}{n_e e} \ , \tag{8}$$

where $p_e = n_e k_B T_e$.

[10] The system of nonlinear Vlasov-fluid equations (1)–(7) permits the existence of circularly polarized Alfvén waves of arbitrary amplitude,

$$\mathbf{B}_w = \frac{1}{\sqrt{2}}\left[B \exp i(k_0 z - \omega_0 t)\mathbf{e}_+ + \text{c.c.}\right] , \tag{9}$$

where the amplitude B is real, and the polarization vector is defined as

$$\mathbf{e}_\pm = \frac{1}{\sqrt{2}}\left[\mathbf{e}_x \pm i\mathbf{e}_y\right],\ (\mathbf{e}_+)^* = \mathbf{e}_- \tag{10}$$

and the plus (minus) denotes right-hand (left-hand) circular polarization. In fact, integrating (3) over the transverse velocity components v_x and v_y, it is straightforward to show that incompressible eigenmodes exist with an ion fluid velocity that is perpendicular to the magnetic field and has the form

$$\mathbf{V}_\perp = -\frac{V_A^2}{(\omega_0/k_0)}\frac{\mathbf{B}_w}{B_0} . \tag{11}$$

The frequency of the pump wave, ω_0, obeys the zeroth-order dispersion relation,

$$Y_0^2 = \frac{X_0^2}{1 \pm X_0} , \tag{12}$$

where $Y_0 = k_0 V_A/\Omega_p$, $X_0 = \omega_0/\Omega_p$, $V_A = B_0/(\mu_0 n_p m_p)^{1/2}$, and $\Omega_p = eB_0/m_p$ is the proton cyclotron frequency.

[11] Perturbations are now considered about an equilibrium that is characterized by the circularly polarized pump wave and a spatially uniform distribution function along the constant magnetic field, which is written as

$$F_0(z, \mathbf{v}, t) = n_0 \delta(\mathbf{v}_\perp - \mathbf{V}_\perp) f_0(v_z) , \tag{13}$$

where the transverse fluid velocity components are given by (11). The linearized Vlasov-fluid equation can thus be expressed as

$$\frac{\partial \delta f}{\partial t} + v_z \frac{\partial \delta f}{\partial z} + \left(\delta E_z + \delta V_x B_y + V_x \delta B_y - \delta V_y B_x - V_y \delta B_x\right) \cdot \frac{\partial f_0(v_z)}{\partial v_z} = 0 . \tag{14}$$

[12] To determine the linear growth or damping of the unstable waves, we assume for simplicity that the perturbation δf varies as $\exp(ikz - i\omega t)$, with a complex frequency ω and a real wave vector k, but in rigor we should use the Landau procedure and take the Fourier-Laplace transform. The expression for δf can be immediately obtained as

$$\delta f = -i\left(\delta E_z + \delta V_x B_y + V_x \delta B_y - \delta V_y B_x - V_y \delta B_x\right)\frac{\partial f_0(v_z)/\partial v_z}{\omega - k v_z} . \tag{15}$$

Following *Hollweg et al.* [1993] (see also *Hollweg* [1994]), the perturbation fields can be expressed as follows:

$$\delta B_\perp = b_+ \exp(ik_+ z - i\omega_+ t) + b_- \exp(ik_- z - i\omega_- t) , \tag{16}$$

$$\delta V_\perp = v_+ \exp(ik_+ z - i\omega_+ t) + v_- \exp(ik_- z - i\omega_- t) , \tag{17}$$

$$\delta E_z = \text{Re}[\varepsilon \exp(ikz - i\omega t)] , \tag{18}$$

where $k_+ = k_0 + k$, $k_- = k_0 - k^*$, $\omega_+ = \omega_0 + \omega$, and $\omega_- = \omega_0 - \omega^*$. The parameter ε denotes the longitudinal electric field amplitude. Linearizing the ion equation of motion (2) then gives

$$v_+(\Omega - \omega_+) = -\frac{e\,b_+}{m_p}\frac{\omega_+}{k_+} + \frac{uB\Lambda}{2} , \tag{19}$$

$$v_-(\Omega - \omega_-) = -\frac{e\,b_-}{m_p}\frac{\omega_-}{k_-} + \frac{u^* B\Lambda}{2} , \tag{20}$$

where $\Lambda = (e\Omega/m_p)(\Omega - \omega_0)$.

[13] For the purposes of the present work, we assume the one-dimensional distribution function f_0 to be Maxwellian. Consequently, from (15) we obtain for the density perturbation the relation,

$$n_1 = \frac{e}{m_p}\left[i\varepsilon + B\left(\alpha\, b_+ + v_-^* - \alpha\, b_-^* - v_+\right)\right]\frac{n_0 Z'(\xi)}{k v_{th}^2} , \tag{21}$$

where Z' is the derivative of the plasma dispersion function [*Fried and Conte*, 1961], with argument $\xi = \omega/kv_{th}$, and v_{th} denotes the parallel thermal speed $v_{th} = (2k_B T_{\|p}/m_p)^{1/2}$, with the parallel proton temperature $T_{\|p}$. The factor $\alpha = V_{\perp 0}/B_{\perp 0}$ is defined by equation (11).

[14] We now evaluate the first velocity moment of equation (14) and obtain the result:

$$\omega u - \frac{k p_1}{m_p n_0} = \frac{e}{m_p}\left[i\varepsilon + B\left(\alpha\, b_+ + v_-^* - \alpha\, b_-^* - v_+\right)\right] . \tag{22}$$

From (14) and (21), and by help of the linearized continuity equation for the density perturbation, we obtain the pressure perturbation p_1 as

$$p_1 = m_p n_1\left[\left(\frac{\omega}{k}\right)^2 - \frac{v_{th}^2}{Z'(\xi)}\right] . \tag{23}$$

[15] Note that by introducing the polytropic coefficient, γ, by means of the usual relation, $\delta p/p_0 = \gamma \delta n/n_0$, gives the kinetic expression:

$$\gamma = 2\left[\xi^2 - \frac{1}{Z'(\xi)}\right] . \tag{24}$$

Since this γ is a complex function of ξ [*Belmont and Mazelle*, 1992], equations (23) and (24) indicate that density and pressure fluctuations will not necessarily be in phase, in

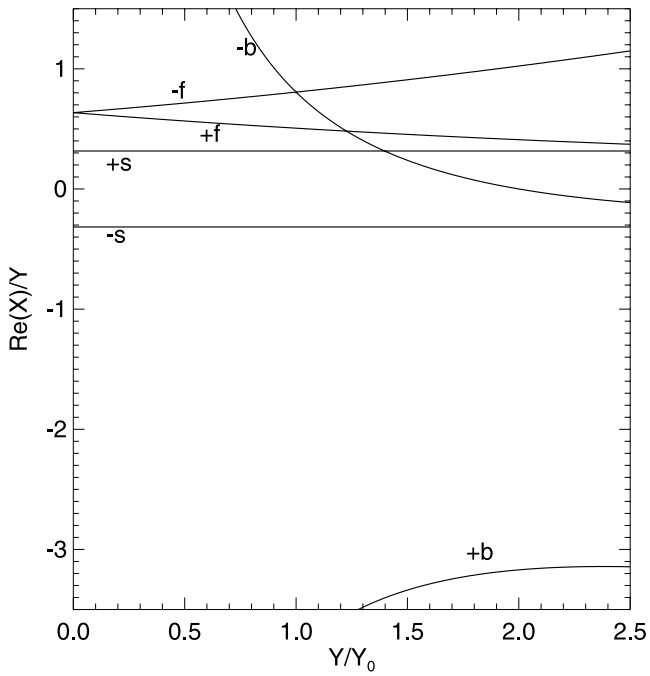

Figure 1. Phase speeds of the six standard ion acoustic-like wave modes, obtained from the kinetic dispersion relation for a left-hand parent wave, as a function of the normalized wave number for $A = 0$, $X_0 = 0.35$, $\beta_e = 0.2$, and $\beta_p \approx 0$.

contrast with the phase-locking that results from the constant value obtained in the fluid treatment. Furthermore, the polytropic coefficient after (24) depends on the dispersion properties of the plasma. Consequently, an inverse Fourier transform of (23) implies an intricated nonlocal real-space relation between pressure and density (whereas in fluids the pressure is a local monomial of the density). Thus kinetic theory introduces nonlocal effects which ultimately control the transfer of energy between the tranverse and longitudinal fluctuations [e.g., *Rogister*, 1971; *Mjølhus and Wyller*, 1988; *Spangler*, 1989; *Hammett and Perkins*, 1990; *Medvedev and Diamond*, 1996]. This explains, in part, why it is not possible to find a reasonable value for γ, when comparing the results from linearized fluid theory with those of the hybrid simulations [*Vasquez*, 1995].

[16] Because we do retain the kinetic effects solely in γ, the dispersion relation preserves the same structure as in the fluid analysis [*Hollweg et al.*, 1993; *Hollweg*, 1994]. Therefore after tedious but straightforward calculations, the dispersion relation can be written in standard form as

$$L_-(L_+D + R_+B_+) + L_+R_-B_- = 0 \ , \tag{25}$$

with the dispersion coefficients,

$$L_\pm = Y_\pm^2 - X_\pm^2/\psi_\pm \ , \tag{26}$$

$$R_\pm = Y_\pm\left(X_0 - \frac{YX_0^2}{Y_0X} + \frac{X_\pm}{\psi_\pm}\right)(2\psi_0)^{-1} \ , \tag{27}$$

$$D = \frac{r}{2}\beta_e Y^2 - X^2\Delta \ , \tag{28}$$

$$B_\pm = \pm\frac{AX\psi_\mp\left(Y_\pm\psi_\pm X_0^2 - Y_0\psi_0X_\pm^2\right)}{Y_0Y_\pm} \ , \tag{29}$$

and with the following definitions,

$$\begin{aligned}
\Delta &= A + r\left(1 - \beta_{pK}Y^2/X^2\right),\\
A &= (B/B_{0z})^2,\\
r &= \psi_0\psi_+\psi_-,\\
\psi_0 &= 1 - X_0;\ \psi_\pm = 1 - X_\pm,\\
X_\pm &= X_0 \pm X;\ Y_\pm = Y_0 \pm Y\\
\beta_e &= p_e/p_B = 2n_ek_BT_e/\left(m_pV_A^2\right),\\
\beta_F &= \beta_e/2,\\
\beta_{pK} &= v_s^2/V_A^2 = (X/Y)^2 - \beta_p/Z',\\
\beta_p &= p_p/p_B = v_{th}^2/V_A^2 \ .
\end{aligned}$$

Here the quantities X and Y represent the normalized values of ω and k, as introduced previously. The above dispersion relation has the same form as that obtained by *Hollweg* [1994]. However, in our case it is not a polynomial equation, and therefore its roots (an infinite number) will not be complex conjugate pairs. Note also that the definition of $\beta(= \beta_e + \beta_p)$ differs from the one used in pure fluid theory β_F because we normalized the particle pressure to the magnetic pressure, $p_B = B_0^2/2\mu_0$, associated with the constant background field. Furthermore, in fluid theory there is no distinction between the electron or proton β, whereas here both are separately considered and the kinetic β_{pK} involves the effective sound speed v_s, as obtained from (23).

[17] In the next section we shall solve this complex dispersion relation numerically, in order to search for damped and growing field-aligned wave modes in the presence of pump waves with left-hand and right-hand polarization.

2.1. Stability Analysis

[18] In order to facilitate the understanding of the kinetic solutions of (25), we first consider a case similar to that described in Figure 1 of *Hollweg* [1994], except that we increased the pump frequency from $X_0 = 0.25$ to $X_0 = 0.35$. Consequently, the pump wave number takes the value $Y_0 = 0.434$. Since $\beta = 0.1$ in that work, we take $\beta = 0.2$ in accord with our definitions, where $\beta = \beta_e + \beta_p$. Figure 1 illustrates the phase speed, Re(X)/Y, of the roots of the dispersion relation (25) as function of wave number normalized by the pump wave number Y/Y_0, for $A = 0$, $\beta_e = 0.2$, and $\beta_p \approx 0$, that is for the fluid case and no pump wave. In this case, (25) attains the simple form, $L_+L_-D = 0$, and the dispersion relation separates into three uncoupled branches.

[19] We show only the six standard modes of (25) (i.e., the two ion-acoustic modes and the four sideband-related ion-acoustic-like modes) because the remaining modes are severely damped. The symbols $+s$ and $-s$ correspond to ion-acoustic modes propagating forward and backward relative to the background magnetic field, respectively.

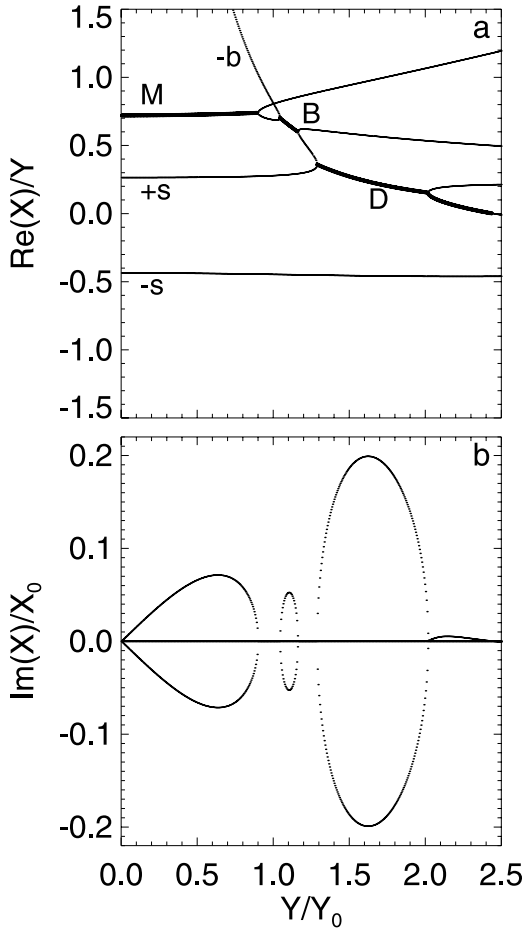

Figure 2. (a) Same as in Figure 1 but now for the case of a finite pump wave amplitude $A = 0.2$. The thick line indicates instability. (b) Growth rate in units of the pump wave frequency versus normalized wave number. Note the appearance of a weakly unstable regime around $Y/Y_0 = 2.0-2.5$.

Those indicated by the symbols $+f$ and $+b$ denote the forward and backward ion-acoustic-like modes driven by the beating of the pump wave and the transverse modes involving the upper sideband frequency and wave number, (ω_+, k_+), respectively. Similarly, the roots denoted by $-f$ and $-b$ correspond to the forward and backward ion-acoustic-like modes related to the transverse waves belonging to the lower sideband, (ω_-, k_-). As has been pointed out by *Goldstein* [1978], it is relevant to recall here that for finite amplitude pump waves the unstable waves will in general not be normal modes of the plasma but driven oscillations or ion quasi-modes.

[20] Figure 2a shows the phase speed, $\mathrm{Re}(X)/Y$, of the roots of (25), where A is increased to 0.2, whereas the other parameters remain unchanged. As is clear from Figure 2a, there are three unstable regions (as indicated by dark lines) which can be recognized by the merging of two roots of the dispersion equation. In this limit, the roots are complex conjugate pairs and correspond to the decay, modulational, and beat instabilities as indicated. Since $\beta_e/2 - 1 + 3X_0 > 0$ and $\beta_e/2 - 1 + X_0 < 0$, this case corresponds, according to the graphical summary of *Hollweg* [1994], to the situation shown in their Figure 18b. Note that the $+b$ mode, because of its uninteresting behavior, was not included in the plot.

[21] Figure 2b shows the growth rate normalized by the pump wave frequency $\mathrm{Im}(X/X_0)$ versus the normalized wave number Y/Y_0. As already observed by *Inhester* [1990] in the pure fluid limit of the decay instability, the roots of the dispersion equation become identical at the edges of the unstable wave number ranges, and consequently we cannot determine which mode goes unstable and which one is damped. Note, however, that due to the small, but otherwise finite, value of β_p a weak unstable region has emerged in the wave number region $2.0 \leq Y/Y_0 \leq 2.5$, without the symmetric damped counterpart.

[22] The degeneracy of the roots in the fluid case can be completely removed if we include collisionless dissipation. In fact, Figure 3a shows again the case with $\beta = 0.2$, but now we have the situation where the electrons are cold, $\beta_e \approx 0$, so that only the ions contribute to the thermal energy, i.e., $\beta_p = 0.2$. Note, first, that the mode structure is completely different from the MHD solutions displayed in Figure 2a. Here, the unstable branches can be clearly

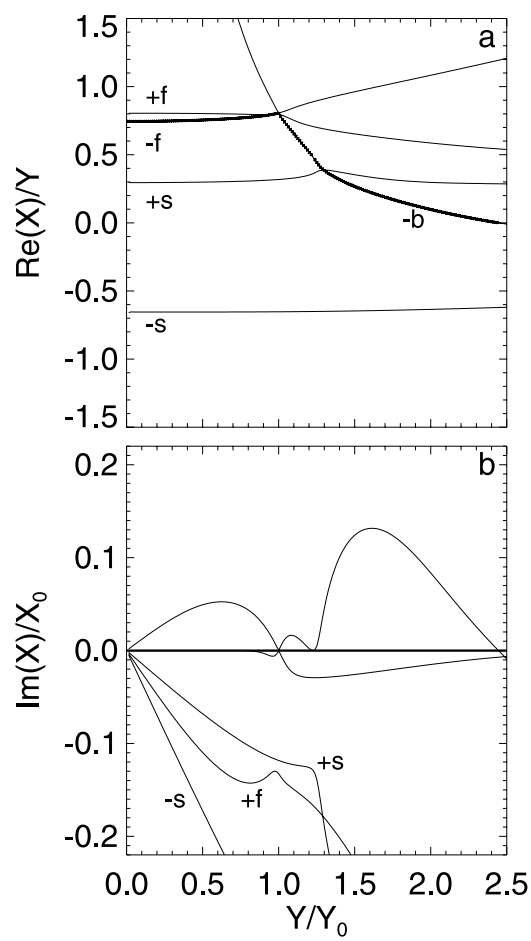

Figure 3. Results as in Figure 2 and for the same total plasma β but now for $\beta_e \approx 0$, and $\beta_p = 0.2$. (a) Phase speeds of the ion acoustic-like modes as a function of the normalized wave number. Note the completely different mode structure and splitting. (b) Growth rate in units of the pump wave frequency versus normalized wave number. Note the extended range of the beat wave instability.

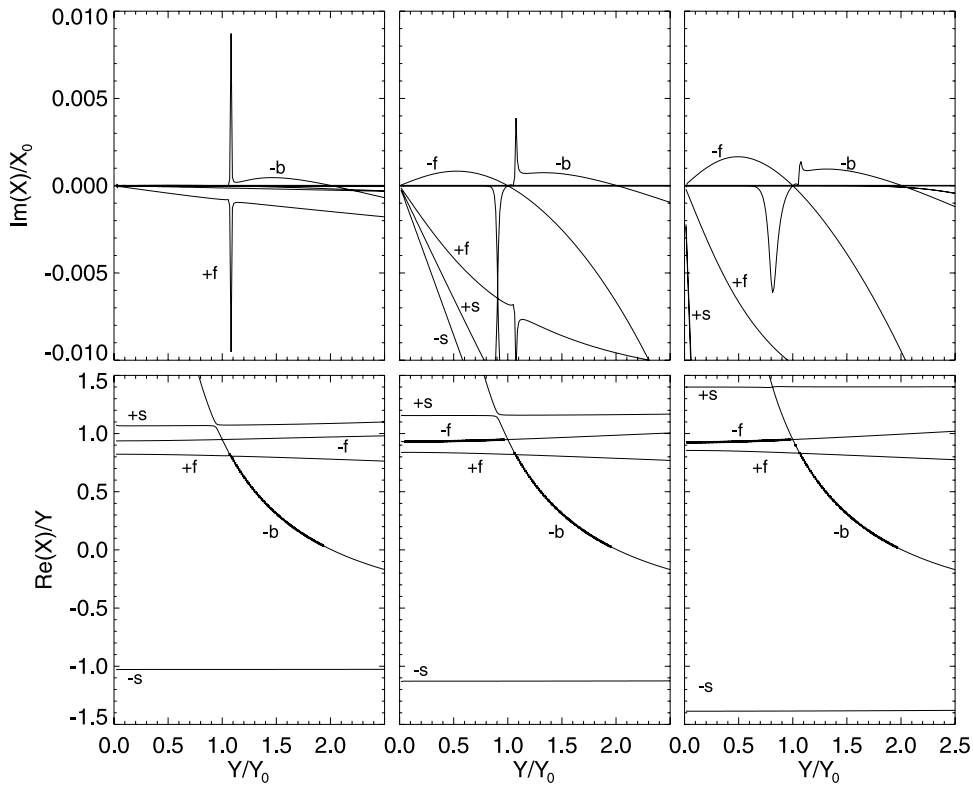

Figure 4. Normalized growth/damping rates (top row) for the various ion acoustic-like modes as function of the normalized wave number, and (bottom row) the corresponding phase speeds. The parent Alfven wave is left-hand polarized with $A = 0.045$. From left to right the proton plasma beta is increased from $\beta_p = 0.08$, to $\beta_p = 0.18$, and finally $\beta_p = 0.5$.

distinguished from the damped ones. In particular, we can observe that the double root of the modulational instability at $Y/Y_0 \leq 1$ in Figure 2a is now split into two roots, one of which, the $-f$ mode, has a positive imaginary part, whereas the $+f$ mode is damped. Similarly, the unstable branch for the decay instability is the $-b$ mode, with decreasing phase speed, and an additional destabilization occurs at $Y/Y_0 > 2.0$, in agreement with *Inhester*'s [1990] results.

[23] Another interesting feature that appears clearly in Figure 3a is the apparent extended range of the decay instability for $Y/Y_0 < 1.2$, actually corresponding to the beat instability arising from the coupling between the $+f$ and $-b$ waves. The beat instability therefore corresponds to an extra destabilization of the $-b$ branch (see Figure 3b). Although in this case the growth rate of the beat instability is relatively small, we shall see that in cases where this instability is dominant, the unstable branch will remain the one of the $-b$ mode. Consequently, and contrary to the fluid results where the beat instability is dominated by the $+f$ sideband, with the wave energy going to high frequencies and wave numbers [*Hollweg*, 1994], the collisionless dissipation will convert the beat instability effectively into a source of backward propagating transverse waves. Qualitative similar results were found by *Gomberoff* [2000] and *Gomberoff et al.* [2001], who introduced a collision-like term in the longitudinal component of fluid equations to simulate the Landau damping. However, a finite set of fluid equations with dissipative terms represents an approximation which may be inadequate for some regimes and $\beta_p \sim 1$. This point has been emphasized by several authors [e.g., *Medvedev and Diamond*, 1996; *Passot and Sulem*, 2004, and references therein].

[24] Let us now discuss in more detail the nature of the different kinetic solutions. Still considering a left-handed pump wave, we again investigate the case with $\beta_e/2 - 1 + 3X_0 > 0$ and $\beta_e/2 - 1 + X_0 < 0$; nevertheless, we choose to start in the fluid regime where the decay instability can be easily stabilized. For example, when taking $\beta_e/2 = 0.8$, $\beta_p \approx 0$, $X_0 = 0.1$, and $A = 0.01$, we obtain a situation where the three instabilities, i.e., modulational, beat, and decay can emerge together. However, if the pump amplitude A is increased the decay mode will be stabilized (see Figures 8a–8c of *Hollweg* [1994]). The modulational instability resulting in this regime, now due to the coupling between the $-f$ and $+s$ waves, might not exist if $\beta_e/2$ 0.9. Consequently, we calculate the roots of (25) with $A = 0.045$ and gradually increase β, by varying β_p and maintaining β_e fixed at $\beta_e/2 = 0.9$. In this way, we can isolate the beat instability in the fluid regime.

[25] Figure 4 examines the consequences of ion kinetics for the above fluid picture. The upper and lower rows show, respectively, the normalized growth rates and phase speeds of the different modes as β_p is increased. The first upper and lower panels of Figure 4 illustrate the case when $\beta_p = 0.08$, so that the fluid plasma $\beta_F \approx (\beta_e + \beta_p)/2$ is approximately 0.94. In this parameter regime a relatively strong beat mode emerges in a very narrow wave number range around $Y/Y_0 \approx 1.1$. Note, nevertheless, the broadening of the

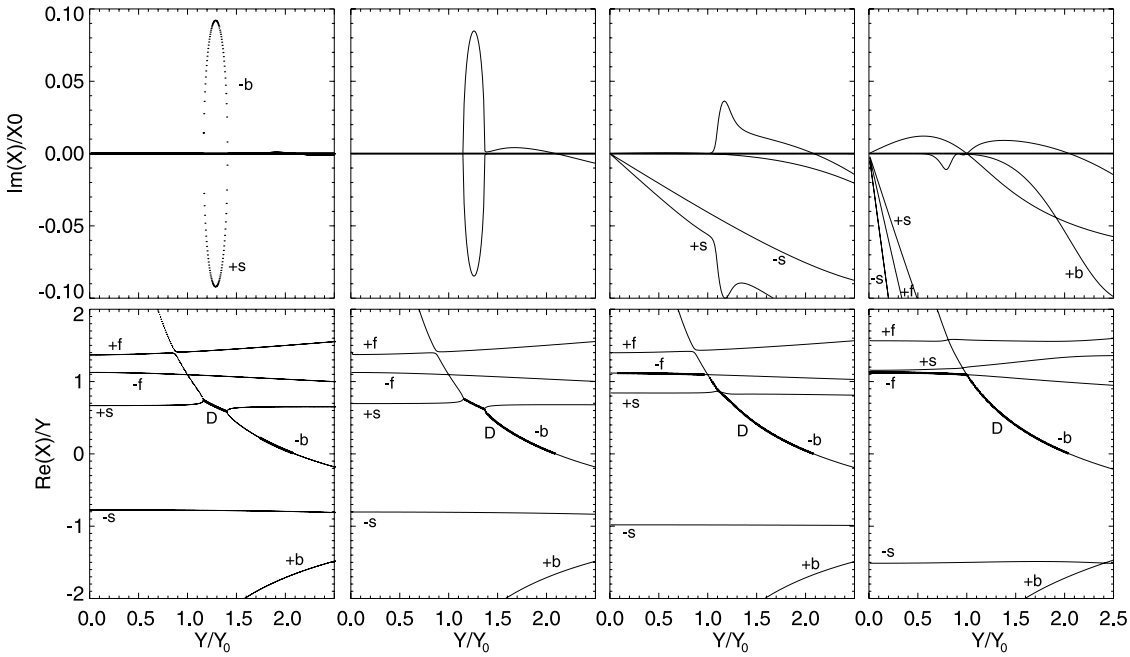

Figure 5. As Figure 4 but for the R mode with $A = 0.2$, $X_0 = 0.2$, and $\beta_e = 1.0$. From left to right the proton plasma beta take the values $\beta_p \approx 0$, $\beta_p = 0.034$, $\beta_p = 0.18$, and $\beta_p = 1.0$, respectively.

instability range, but at much smaller growth rates due to the interaction of the wave with a small population of resonant ions (the thermal speed is still too low, $v_{th} \approx 0.24V_A$).

[26] This instability should not be confused with the decay instability which, as already shown by *Inhester* [1990] and at the beginning of this section, exhibits a similar behavior. In fact, the $-b$ mode in this case has a monotonically decreasing phase speed, and the unstable range, for $\beta_p \neq 0$, has an upper bound at $Y/Y_0 \approx 2.0$. However, as we already know, this instability results from the coupling of the $-b$ and $+f$ waves. The latter mode has a relatively constant phase speed and exhibits an enhanced Landau-damped rate in the coupling region, which resembles the fluid symmetric solutions at $\beta_p = 0$. The ion quasi-modes $+s$ and $-s$ have also a constant phase speed, but they are only slightly damped. The diagrams in the middle panels of Figure 4 display the case of β_p being increased to $\beta_p = 0.18$. The maximum growth rate of the beat instability is now about 50% of the maximum in the first diagram (about 30% of the maximum growth rate in the fluid limit). However, the $-f$ mode now has become unstable, giving rise to a modulational instability in the wave number range $Y/Y_0 \approx 0-1$, with growth levels comparable to the broadened unstable region of the beat mode, whereas the remaining modes become progressively more Landau-damped.

[27] For $\beta_p = 0.5$, the last two panels show that the modulational instability might even be the dominant instability, with the $-f$ mode reaching larger growth rates on a broader wave number range than the $-b$ wave. This modulational instability is in agreement with the one predicted by *Mjølhus and Wyller* [1988], *Spangler* [1989], and *Medvedev et al.* [1997] using the kinetically modified DNLS equation, and from numerical simulations based on a dispersive Landau-fluid model [*Bugnon et al.*, 2004].

[28] If A is increased further, the beat instability will be enhanced (as it occurs in the fluid regime) so that both the beat and modulational instabilities may be simultaneously present in the system. However, the beat mode tends to have a larger growth rate than the modulational instability, and it is the dominant instability for large-amplitude pump waves.

[29] As previously mentioned, in the fluid regime the modulational instability can also result from the coupling between the $-f$ and $+s$ waves when $\beta_F \approx 1$ [*Hollweg*, 1994], in contrast to the usual situation where instability is due to the interaction between the $+f$ and $-f$ modes. Here again, kinetic effects break the degeneration of the coupled modes. As a result, the $-f$ mode becomes unstable whereas the $+s$ is damped. Therefore the conclusion drawn from all these cases that refer to the left-handed pump wave is that the only modes which can becomes unstable are the $-f$ and $-b$ modes.

[30] We turn now our attention to the right-hand (R-mode) pump wave. In the fluid regime a right-handed wave can undergo either the beat, decay, and/or the modulational instability, depending sensitively on the values of the plasma β_F and the pump amplitude. The beat and decay instabilities cannot emerge together, and the beat exists only when the pump amplitude exceeds a threshold value. Furthermore, if $\beta_F \gtrsim 1$ the beat instability will be the only remaining mode, if the pump amplitude is large enough to quench the modulational instability [*Hollweg*, 1994].

[31] Figure 5 illustrates the case in the fluid regime where the decay instability is more important than the beat instability. Specifically, we choose the constraints, $\beta_e/2 - 1 - 3X_0 < 0$ and $\beta_e/2 - 1 - X_0 < 0$, with $\beta_e/2 = 0.5$, $X_0 = 0.2$, and $A = 0.2$, which correspond to the fluid conditions of the graphical summary in Figure 18d of *Hollweg* [1994]. Note that we are using positive pump frequencies (and also positive pump wave numbers) so that the above relations have a negative sign in front of X_0 as compared with those in Hollweg's work.

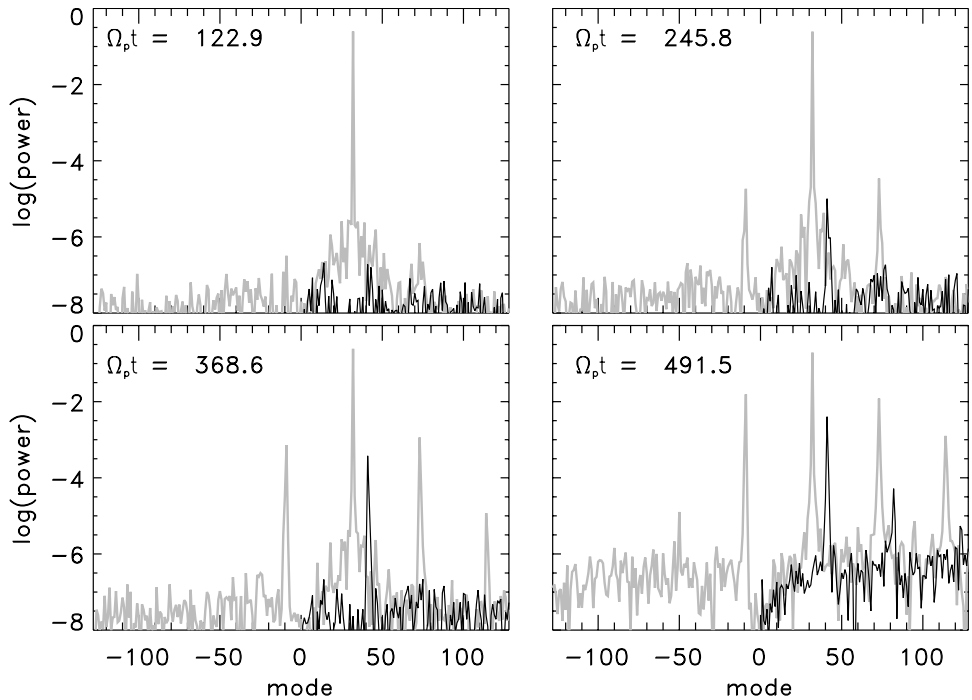

Figure 6. Time evolution of the power spectrum for the magnetic field fluctuations (gray line) and density fluctuations (dark line) as function of the mode number for the L mode parent wave. The pump amplitude B is 0.5, m = +32, β_e = 1.4, and β_p = 0.01.

[32] The first diagram shows the case when $\beta_p \approx 0$ so that the fluid plasma beta is $\beta_F \approx 0.5$. The decay instability appears, as expected from the chosen fluid regime, as a consequence of the coupling between the $+s$ and $-b$ waves. Note that the phase speeds of the $\pm s$ modes are given approximately by $c_{\pm s} = \pm\beta^{1/2}{}_F$. Again, a small increase of the ion temperature (β_p = 0.034) is enough to break the symmetry in the complex plane, and to make the $-b$ branch recognizable as the unstable mode. As it follows from the remaining diagrams of Figure 5, the effect of increasing further the ion plasma β_p reflects in a significant reduction of the growth rate of the decay instability but also in a broadening of the instability wave number range.

[33] At β_p = 0.18, the third diagram shows that the $-f$ mode is just starting to be excited in the form of a modulational instability (as indicated by the dark line on the phase speed plot), whereas the ion quasi-modes $\pm s$ become increasingly Landau-damped. At thermal equilibrium between protons and electrons, the phase speed of the $-s$ mode is slightly larger than that of the $-f$ mode but nevertheless, it is strongly Landau-damped as well. The modulational instability reaches a larger growth rate than the decay instability; however, the maximum is only at about 15% of the maximum growth rate of the decay instability in the first diagram. At larger pump amplitude, however, the decay instability tends to dominate the modulational instability so that only under the condition $\beta_p > \beta_e$ the modulational instability may attain similar growth levels than the decay instability.

3. Hybrid Model

[34] In order to investigate the time evolution of the instabilities and to verify the linear analysis described above, we have performed a number of high-resolution and low-noise simulations using a hybrid code that is one-dimensional but retains all three vector components of the magnetic field and particle velocities [e.g., *Winske and Leroy*, 1984; *Terasawa et al.*, 1986]. In the simulations, electrons are considered as a massless and isothermal fluid, whereas the protons are treated kinetically as discrete particles representing a homogeneous, magnetized, collisionless plasma. The particle equations are advanced in time with a leapfrog method, and the moments are computed with a second-order weighting scheme. The fields are advanced in time explicitly, and their derivatives are computed from a fourth-order finite difference scheme. For the high-resolution studies, the simulation box length has been chosen as 32 times the wavelength of the pump wave, with 2048 grid cells and 400 particles per cell. The time step used is typically $\Delta t\Omega_p^{-1}$ = 0.01–0.03, where Ω_p is the proton gyrofrequency. The boundary conditions are periodic for both particles and fields, and the background magnetic field $\mathbf{B}_0$ is in the z direction.

[35] We initialize the simulations with a uniform wave train so as to represent the parallel propagating circularly polarized Alfvén pump wave (7) of a given polarization. The initial velocities of the simulation particles are so assigned that they have a given parallel thermal speed v_{th} and a transverse bulk velocity $\mathbf{V}_\perp$ given by (11). In order to facilitate the comparison with the fluid theory and previous kinetic studies, we choose pump wave parameters similar to those used by *Terasawa et al.* [1986] and *Vasquez* [1995]. Therefore the pump wave number is k_0 = 0.408 and consequently the L (R) mode has values ω_0 = 0.333 (0.499).

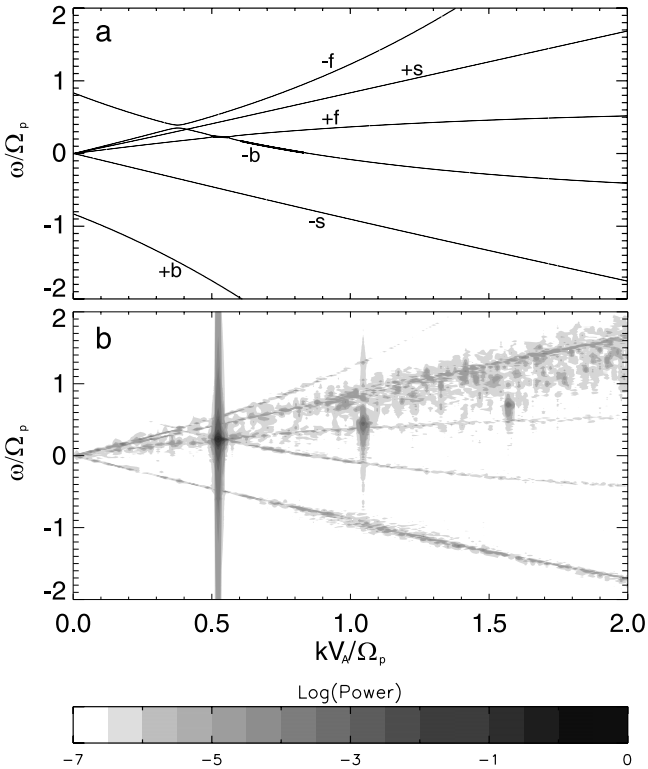

Figure 7. (a) Dispersion roots for the L mode with β_p = 0.01. (b) Power spectrum ($\omega - k$ diagram) of density fluctuations for the L mode parent wave in the same format as in Figure 7a. The gray scale denotes the wave power in logarithmic scale.

3.1. L-Mode Simulations

[36] The nature of the parametric instabilities in general depends not only on the pump wave amplitude and on β but also on the ratio β_p/β_e, i.e., on the temperature ratio, T_p/T_e. In order to get further insight into the role of ion kinetics, it is important to verify and make sure that instabilities in the kinetic and fluid descriptions do substantially differ. As mentioned in the previous sections, the fluid part of the instabilities has, in general, a strong dependence on β_e and thus, when comparing hybrid simulations with pure fluid theory, the most appropriate beta value to use in the fluid dispersion relation is not β. Instead, β_e should be used. By taking β = 1.5 and T_i/T_e = 0.5 in his simulation of the L mode, *Vasquez* [1995] concluded that the predominantly M-type instability was not to be expected from pure fluids, where only a beat instability occurs for β = 1.5. However, if β_e (actually $\beta_F = \beta_e/2$) is used in the fluid theory, a strong modulational instability and much more weaker and narrower-band beat and decay instabilities emerge. On the other hand, increasing β_p from zero to β_p = 1/3 (note that $T_i = 3\beta_p/2$ in Vasquez's work) in the kinetic dispersion relation (25), the effect of Landau damping reduces the growth rates and broadens the wave number range of the beat instability (the decay will almost disappear). Consequently, in order to isolate effectively the beat instability in the fluid regime and to show the effects of ion kinetics, we have chosen a larger pump wave $B = 0.5B_0$ and increased β_e from β_e = 1.0 to 1.4 [see *Hollweg*, 1994, Figure 18c]. Therefore in our subsequent study, β_p is gradually increased from $\beta_p \approx 0$ to finite values.

[37] Figure 6 shows a time sequence of the wave power in the magnetic field fluctuations (gray line) and density fluctuations (dark line) as a function of the mode number m, for the fluid case (β_p = 0.01). At relatively early times ($t \approx 122\Omega^{-1}{}_p$), the parent Alfvén wave is responsible for the peak at mode m = +32, whereas the signal-to-noise ratio is too small yet to allow one to distinguish a growing mode. Around $t = 245\Omega^{-1}{}_p$, the magnetic wave power residing at modes m = −9 and m = +73 is apparent, corresponding to the backward-lower and forward-upper sideband waves (ω_-, k_-) and (ω_+, k_+), respectively. The density fluctuation power peaks at mode m_d = +41, indicating what could be the growth of a beat instability. On the other hand, the growth of high-order sidebands in the magnetic-field fluctuation power at $m = 32 \pm m_d$ and $m = 32 \pm 2\ m_d$, and for the density at $m = 2\ m_d$ and $m = 3\ m_d$ in the weakly nonlinear regime is evident in the last panel, in agreement with the results from the weakly nonlinear fluid theory and the MHD simulations by *Hoshino and Goldstein* [1989]. Furthermore, note the preference for the generation of forward propagating transverse waves [*Hollweg*, 1994].

[38] Let us now consider in more details the mode structure by examining the density fluctuations in frequency

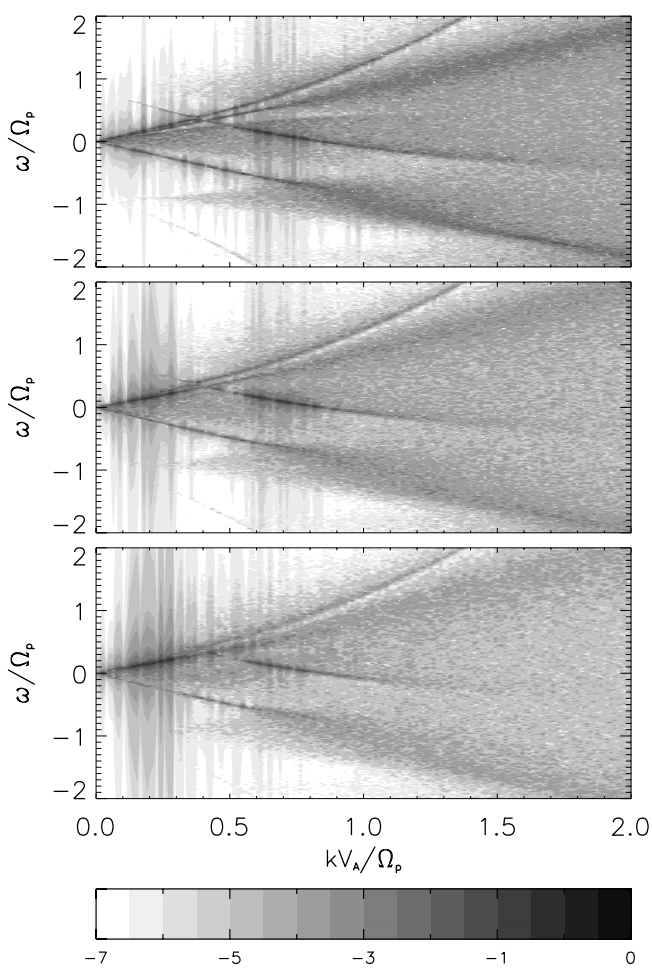

Figure 8. $\omega - k$ power spectra in the same format as Figure 7, but from the simulations for the L mode with (top) β_p = 0.1, (middle) β_p = 0.22, and (bottom) β_p = 0.3.

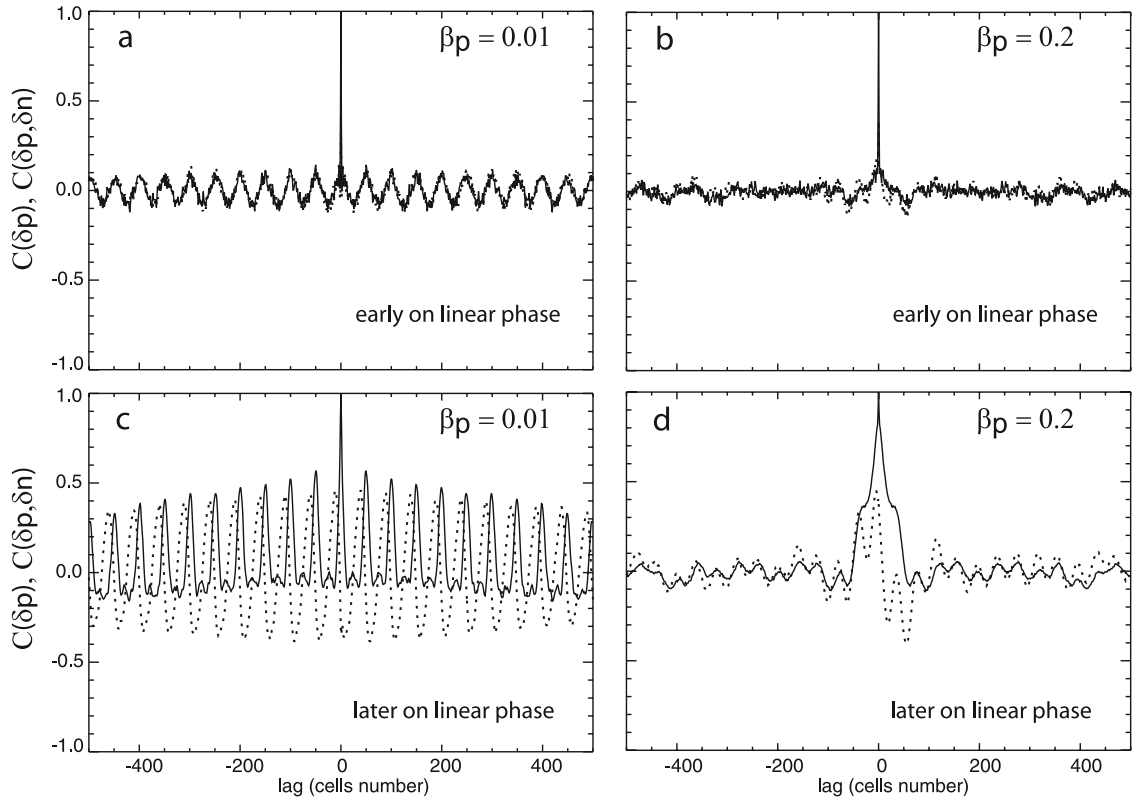

Figure 9. Autocorrelation of the pressure fluctuations $C(\delta p)$ (solid line) and cross-correlation between density and parallel pressure fluctuations $C(\delta p, \delta)$ (dashed line) during the linear phase of the instability of the L mode parent wave.

as well as in the wave number space. Figure 7 displays the dispersion relations as calculated from the simulation and from the linear theory, and shows the $\omega - k$ dispersion relation obtained by Fourier-transforming, both in space and time, the density fluctuations during the initial phase of the instability. The gray scale denotes the wave power on a logarithmic scale. It is clear that most of the wave power resides at $\omega \approx 0.23$ and $k \approx 0.52$, corresponding to the position where the $+f$ and $-b$ branches of the theoretical dispersion curves intersects (Figure 7a). This confirms that the matching conditions and dispersion properties for the beat instability in the fluid regime are satisfied. Figure 7 also reveals that the linear prediction very well corresponds to the spectrum observed in the simulation, allowing a complete identification of the remaining modes. Furthermore, note that the $+b$ mode is damped.

[39] Let us now investigate the effects of ion kinetics by increasing β_p. Figure 8 displays the power spectrum of the density fluctuations which were obtained from a set of three simulations with the same plasma configuration as in Figures 6 and 7, except that here β_p was gradually increased. The top panel shows the result for $\beta_p = 0.1$. Comparing with Figure 7 it is evident that even for a small but finite value of β_p, the kinetic plasma response significantly differs from the pure fluid behavior. The beat instability is now localized on the $-b$ branch, exhibits a broad spectrum, and is shifted with respect to the maximum of the fluid case (the type-D instability in Vasquez's work). Note that due to the higher thermal noise level, the harmonic modes are blurred or Landau damped. The middle panel shows the case for $\beta_p = 0.22$. We observe that the $-f$ branch is becoming unstable at $k < k_0$ which, according to with the kinetic theory, corresponds to the modulational instability. The last panel shows that for $\beta_p = 0.3$ most of the density wave power resides on the $-f$ branch, indicating the dominance of the modulational instability over the beat instability. In the fluid regime, however, exactly the opposite occurs for these parameters, while the beat instability still has its peak in a narrow band around $k \approx 0.52$.

[40] When the pump amplitude is increased to $B = 0.6$, it is observed that the beat instability can reach a growth rate that is comparable to the modulational one. For $B = 0.7$, the modulational instability is still present, but only by a significant increase of the proton plasma β_p can the modulational instability acquire a more prominent growth rate. For larger pump amplitudes the beat instability becomes clearly dominant, in agreement with the kinetic analysis of the previous section. Since the modulational instability emerges only in the presence of ion wave dispersion, Alfvén waves could be modulationally unstable only for high-frequency waves, that is to say, for the ion-cyclotron frequency regime and small-to-moderate amplitude of the pump wave. However, for pump frequencies lower than the ion-cyclotron frequency the kinetic effects are, via Landau damping and particle trapping, still operative, and the $-b$ mode will remain unstable as described.

[41] It is worthwhile to make a complementary examination, in order to appreciate when kinetic effects are expected to be important. Figure 9 shows the auto-correlation of the

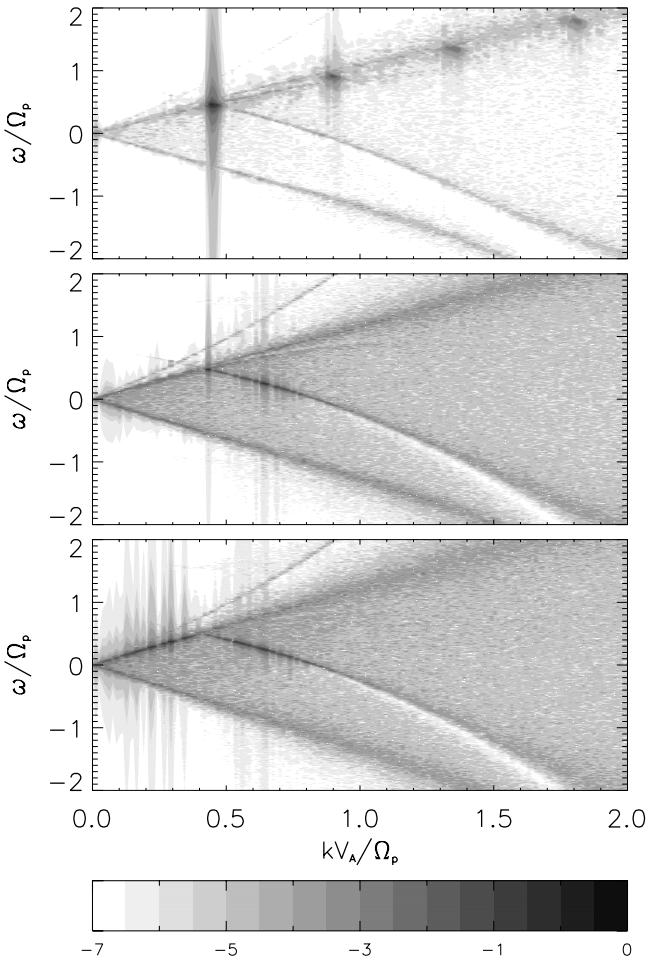

Figure 10. The $\omega - k$ diagrams in the same format as Figure 8 but for the R mode with (top) $\beta_p = 0.1$, (middle) $\beta_p = 0.2$, and (bottom) $\beta_p = 0.3$.

pressure, C(δp), and cross-correlation between density and parallel pressure fluctuations, $C(\delta p, \delta n)$, for early and late stages of the linear evolution of the L-mode, for the cases with $\beta_p = 0.01$ and $\beta_p = 0.2$. As can be seen from Figure 9a, during the early linear stage of the instability, the low-β_p case exhibits both C(δp) and $C(\delta p,\delta n)$ values which clearly indicates coherent effects of periodic structures. When the fluctuations have grown enough (as shown in Figure 9c), the periodic structures are clearly visible but with a significant dephasing between the fluctuations in pressure and density. This particular result clearly suggests that kinetic effects cannot be ignored even within the fluid regime, which is contrary to the traditional belief. For the case with $\beta_p = 0.2$, the thermal effects suppress the early formation of such coherent correlations and manifest itself in a weak dephasing between the density and pressure fluctuations in the region of the largest pressure autocorrelation (Figure 9b). Finally, in the later stage of this case (Figure 9d), we observed that within the region where the pressure fluctuations are strongly auto-correlated, the cross-correlation exhibit sudden changes, between positive and negative values, which indicates a significant decorrelation effect. Thus we see clear evidence for the predictions of section 2 that density and pressure fluctuations will not necessarily be in phase, and for the idea that the polytropic index depends on the instantaneous state of the plasma. Moreover, we have observed that before saturation occurs, the distribution function undergoes strong topological changes in velocity space that cannot be accounted via a lineal treatment because the interactions of the charged particles with the growing ion-acoustic waves is actually a nonlinear problem. These effects breakdown the symmetry of the distribution function mainly in the direction parallel to the magnetic field and they are even stronger for $\beta_p \ll 1$. Thus ironically and in consequence, the regime just where the fluid theory appears to be most appropriate, is also where the kinetic effects play the most dominant role in the saturation mechanism and determines the spectral energy transfer for the postsaturation stage.

3.2. R-Mode Simulations

[42] Let us now describe the results of the simulations for the right-hand polarized pump wave. According to the fluid theory, if the parameter regime satisfies the constraints $\beta_e/2 - 1 - 3X_0 < 0$ and $\beta_2/2 - 1 - X_0 < 0$ the only instability is the decay instability [see *Hollweg*, 1994, Figure 18d]. Thus to examine the effects of ion kinetics on the decay, we choose $\beta_e = 2.0$, a pump amplitude of $A = 0.5$, and gradually increase β_p from zero, to finite values, but restricting β so that the above conditions be still satisfied.

[43] Figure 10 shows the $\omega - k$ dispersion relation of the density fluctuations in the linear stage for the cases $\beta_p = 0.1$, $\beta_p = 0.2$, and $\beta_p = 0.3$, respectively. As expected from the linear theory for a finite-amplitude pump wave, the top panel shows that in the low β_p regime ($\beta_p = 0.1$), the decay instability is dominant and leads to the generation of several harmonics. Most of the power resides in $\omega \approx 0.45$ and $k \approx 0.45$, corresponding to the region where the $+s$ and $-b$ mode merge and therefore giving rise to the decay instability. It is important to point out that for finite pump amplitude the $+s$ mode couples with the $-f$ mode in the unstable region ($k/k_0 \lesssim 1$). At large k, however, the $-f$ mode is quickly damped whereas the $+s$ mode extends a little more (although weakly). The reason for this behavior is that the $+s$ (and also the $-s$) wave, as normal modes, can get slightly excited due to the thermal noise, however the $-f$ mode cannot because it is an ion quasi-mode.

[44] The middle panel shows the result for $\beta_p = 0.2$. The decay instability is still present but the peak intensity is weaker compared with that of the first case. In addition, we observe a destabilization of the $-b$ mode at $k/k_0 \gtrsim 1.5$ and the quench of the harmonics, as also seen in the previous section for the L-mode case. The last panel shows that for $\beta_p = 0.3$ most of the density wave power resides on the $-b$ mode and also at $k < k_0$, indicating the presence of a modulational instability. According to kinetic theory, this destabilization occurs on the $-f$ branch, whereas the $+s$ mode is damped (except for the weak excitation due to the thermal noise). Note also that there is a broadening of the unstable wave number ranges and no power on the original position of the decay instability. In the fluid regime, the modulational instability cannot emerge for these parameters and the decay instability still exists around $k \approx 0.45$.

[45] Figure 11 shows a time sequence of the wave power in the magnetic field fluctuations (gray line) and density fluctuations (dark line) as a function of mode number m, for

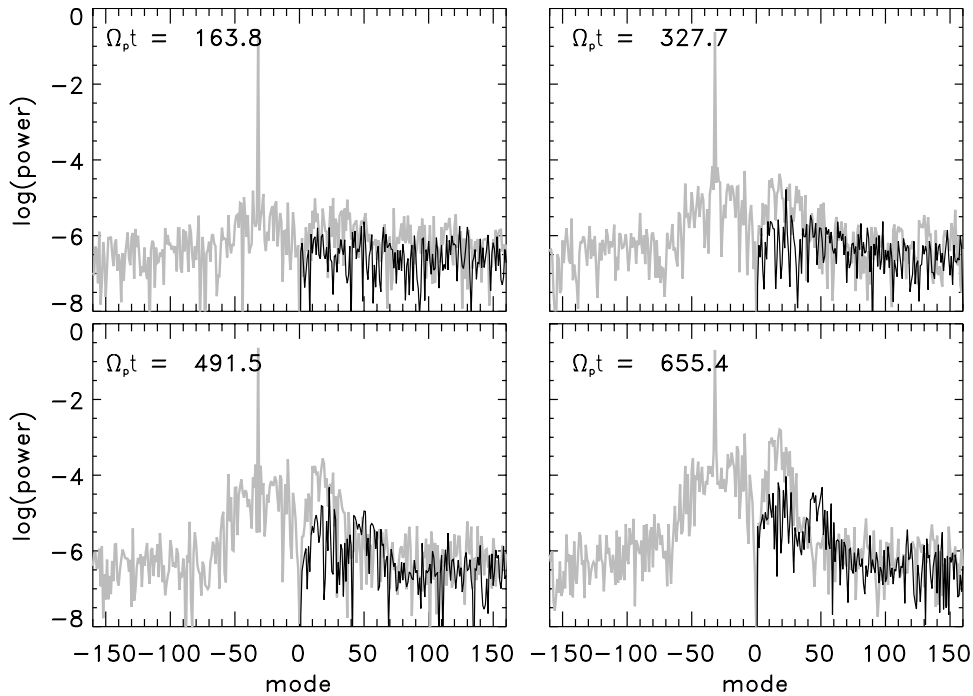

Figure 11. Plots similar to Figure 6 show the evolution of the R mode for the case with $\beta_p = 0.3$. The parent Alfvén wave has $m = -32$ and is propagating forward.

the case ($\beta_p = 0.3$). Since the pump wave is right-hand polarized, magnetic wave power at $m < 0$ corresponds to transverse fluctuations propagating forward. Thus the parent Alfvén wave has $m = -32$. Around $t \approx 492\ \Omega_p^{-1}$, magnetic power residing at modes $m \approx -9$ and $m \approx -55$ is already evident, corresponding to the forward-lower ($-f$) and forward-upper ($+f$) sideband waves, respectively. Because density fluctuation power peaks at $m_d \approx 23$, the resonant condition for a modulational instability is satisfied. On the other hand, the growth of magnetic field fluctuation power at $m \approx 19$, and for the density at $m_d \approx 50$, indicates the presence of the decay instability. At the end of the linear stage ($t \approx 655\ \Omega^{-1}{}_p$), most of the magnetic power is seen at $m \approx -9$ and $m \approx 18$. This confirms the predictions of the kinetic theory, namely that the modulational and decay instabilities are dominated by the $-f$ and $-b$ modes, respectively.

[46] Figure 12 shows the measured growth rates of the unstable density fluctuation modes for the three cases studied. For $\beta_p = 0.1$, the strong peak at $k \approx 0.45$ in the top panel of Figure 11 corresponds to the growth rate of the decay instability, while the secondary peaks correspond to the growth curves of the compressional harmonic waves. The growth rate of the decay instability is approximately at 75% of the calculated kinetic linear rate. When β_p is increased to $\beta_p = 0.2$, the middle panel shows an abrupt reduction of the growth rate of the decay instability. As already noted in Figure 10, not only the harmonic waves are damped but so is the background noise wave activity, which notoriously is quenched at $k > 1$. The growth rate of the peak of the decay instability in this case is about 72% smaller than in case a and amounts to about 45% of the calculated linear rate.

[47] Another important feature of Figure 12 (middle) is the growth at $0.5 \lesssim k \lesssim 0.8$, corresponding to the additional destabilization of the $-b$ mode. The linear kinetic theory and simulations gives the same growth rates for this wave number region. Finally, the growth rates for $\beta_p = 0.3$ are shown in the bottom panel. Here, both kinetic instabilities, decay and modulation, are present but the growth rate of the modulational instability is slightly larger. The calculated kinetic linear rates exhibit exactly the same behavior, but the growth rate corresponding to the modulational instability is about 50% larger than the one computed from the simulation. Similar discrepancies for the modulational instability appear for the growth rates for a pump wave with a larger frequency ($X_0 = 0.6$). Nevertheless, the instabilities can still be clearly identified. This discrepancy may be due to the fact that our Vlasov-fluid model does not include ion-cyclotron damping. In fact, the dispersive effects arising from the cyclotron motion in our model partially retain the fluid-like character of the MHD description. Furthermore, finite-Larmor-radius (FLR) corrections were not included. To properly incorporate the FLR effects would require that the determination of the first-order distribution be obtained by integrating the equilibrium distribution along the characteristics (the unperturbed trajectories). In the presence of a single monochromatic finite-amplitude Alfven wave, this is a formidable task since the trajectory equations give rise to elliptical integrals [*Roberts and Buchsbaum*, 1964] which have to be incorporated in the linear analysis. In the case of a small-amplitude pump waves, the method of *Lee and Kaw*, [1995] could be adapted to obtain a solution that can be compared with recent fluid-kinetic models that use more sophisticated closure schemes. However, as remarked by *Vasquez*, [1995], particle and even fluid simulation growth rates are influenced by several effects, including weak

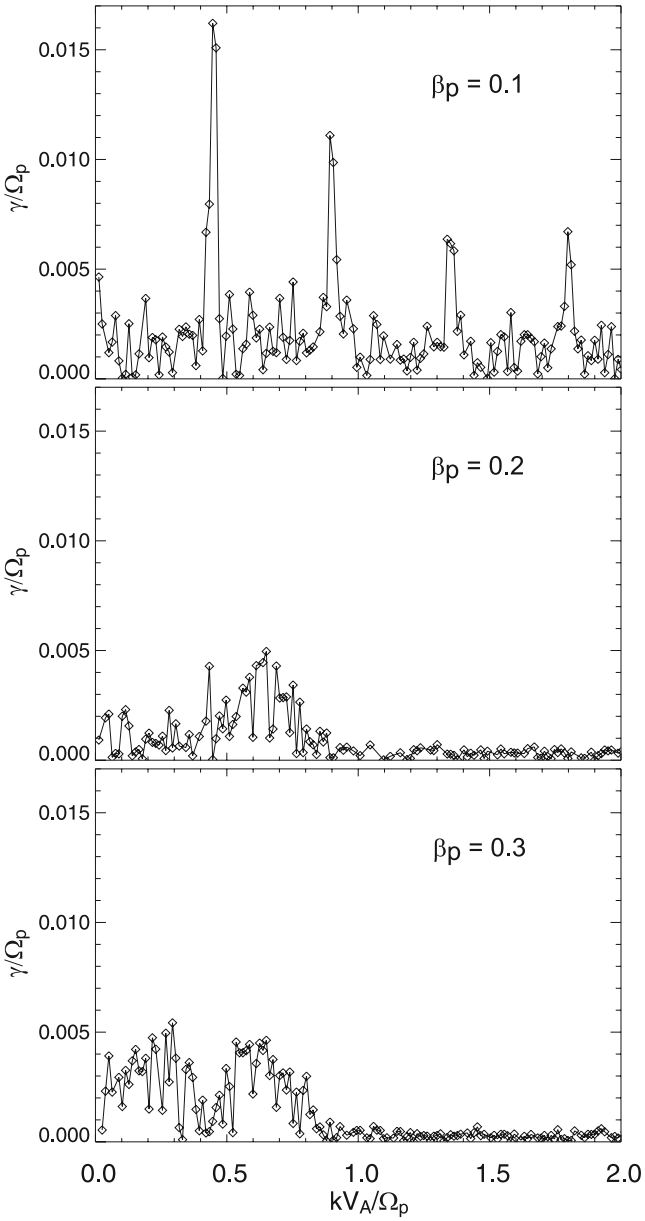

Figure 12. Growth rates of the unstable density modes as a function of the normalized wave number for the R mode. The proton plasma beta is (top) $\beta_p = 0.1$, (middle) $\beta_p = 0.2$, and (bottom) $\beta_p = 0.3$. Note the abrupt decrease of the main peak of the MHD-decay instability's growth rate for increasing β_p.

nonlinear couplings in the linear regime. Therefore simulations and linear-mode calculations do not generally give exactly the same growth rates.

4. Conclusions

[48] We derived from a Vlasov-fluid model a set of equations that describe the parametric instabilities of circularly polarized Alfvén waves of arbitrary amplitude in an electron-proton plasma with kinetic effects. The dispersion relation was numerically evaluated by using a self-consistent distribution function. An examination of the mode structure of the ion acoustic-like waves for both left- and right-hand polarized pump waves was presented. Our analysis and simulations show that even at relative low β_p ($\beta_p \sim 0.1$) kinetic effects break the degeneracy of solutions as obtained in the the standard picture of fluid-mode coupling, thus allowing us to identify unambiguously the growing and damped modes. Our linear-mode calculations complement the drift-kinetic study of the decay instability by *Inhester* [1990], who showed that a small amount of ion thermal energy not only leads to a drastic reduction of the maximum growth rates of the instability as compared to the fluid limit but also shifts the wave number of the maximum growth rate and broadens the unstable wave number range.

[49] We also found that the beat instability exhibits a similar behavior, and that for both instabilities (i.e., the beat and decay) the unstable branch is the $-b$ mode. Although an enhancement of β_i decreases the growth rates of these instabilities, collisionless dissipation leads to the excitation of ion quasi-modes and to the generation of backscattered Alfvén waves. Since the condition $\beta_p \gtrsim 0.1$ is fulfilled most of the time in the solar wind plasma, the beat and decay instabilities may be an effective mechanism to generate backward propagating Alfvén waves. They have been invoked to play a key role in the local production of turbulence and reduction of the cross helicity in the solar wind, and in the pitch-angle diffusion [see *Marsch and Tu*, 2001] of the core protons in the velocity distributions of the fast solar wind. We suggest that using high time resolution solar wind plasma data of proton density and pressure, for example as those in the 3DP plasma detector in the WIND spacecraft which resolves the distribution function in 3 s with a telemetry time of perhaps 12 s, a cross-correlation between these quantities could be carried out to search for events where the dephasing of density and pressure is observed and if possible to examine the shape of the proton distribution function during those times. Another observational signature for the presence of the ion acoustic-like waves and the dephasing effect should be a quasi-monochromatic bump in the density spectrum and its correlation with the magnetic power spectrum as studied by *Agim et al.* [1995] and *Spangler et al.* [1997]. On the basis of the results of this paper the analysis carried out, for example, by *Spangler et al.* [1997], should be performed using kinetic theory. This will help to verify that kinetic effects are certainly important even in low β_p plasmas. We speculate that kinetic effects are also important in regions such as the solar corona where β_p has been estimated to be very small ($\sim$0.001) and where most of the studies has been carried out using fluids models with little or no kinetic effects included.

[50] The results found in the present paper are limited to the cases where strong nonlinearities could be neglected. Thus the nonlinear saturation and long-time evolution of the instabilities were not considered [*Vasquez*, 1995]. Our results are also limited to one spatial dimension. The extension of this study to a two-dimensional model would enlarge the parameter space, and therefore allow more mode-couplings and excited waves to be oblique [*Viñas and Goldstein*, 1991a, 1991b]. We are currently examining such scenarios, and a detailed discussion will be presented in a separate article.

[51] **Acknowledgments.** This work was partially supported by the University of Concepción grant DIUC 204.011.035-1.0. J. A. Araneda

gratefully acknowledges the hospitality of the Max-Planck-Institut für Sonnensystemforschung, Katlenburg-Lindau, Germany. A. F. Viñas thanks the NASA Wind/SWE Program at GSFC for his support.

[52] Amitava Bhattacharjee thanks Dan Winske and another reviewer for their assistance in evaluating this paper.

References

Agim, Y. Z., A. F. Viñas, and M. L. Goldstein (1995), Magnetohydrodynamic and hybrid simulations of broadband fluctuations near interplanetary shocks, *J. Geophys. Res.*, *100*, 17,081.

Araneda, J. A. (1988), Parametric instabilities of parallel-propagating Alfvén waves: Kinetic effects in the MHD-model, *Phys. Scr. T*, *75*, 164.

Belcher, J. W., and L. Davis (1971), Large-amplitude Alfvén waves in the interplanetary medium, 2, *Geophys. Res. Lett.*, *76*, 3534.

Belmont, G., and C. Mazelle (1992), Polytropic indices in collisionless plasmas: Theory and measurements, *J. Geophys. Res.*, *97*, 8327.

Brodin, G., and L. Stenflo (1988), Three-wave coupling for MHD plasmas, *J. Plasma Phys.*, *39*, 277.

Bruno, R., and V. Carbone (2005), The solar wind as a turbulence laboratory, *Living Rev. Sol.*, *2*, (Available at http://www.livingreviews.org/lrsp-2005-4.)

Bugnon, G., T. Passot, and P. L. Sulem (2004), Landau-fluid simulations of Alfvén-wave instabilities in a warm collisionless plasma, *Nonlin. Proc. Geophys.*, *11*, 609.

Derby, N. F. J. (1978), Modulational instability of finite amplitude circularly polarized Alfvén waves, *Astrophys. J.*, *224*, 1013.

Forslund, D. W., J. M. Kindel, and E. L. Lindman (1972), Parametric excitation of electromagnetic waves, *Phys. Rev. Lett.*, *29*, 249.

Fried, B. D., and S. D. Conte, (1961), *The Plasma Dispersion Function*, Elsevier, New York.

Ghosh, S., A. F. Vinas, and M. L. Goldstein (1993), Parametric instabilities of a large-amplitude circularly polarized Alfven wave: Linear growth in two-dimensional geometries, *J. Geophys. Res.*, *98*, 15561.

Goldstein, M. L. (1978), An instability of finite-amplitude circularly polarized Alfvén waves, *Astrophys. J.*, *219*, 700.

Gomberoff, L. (2000), Ion acoustic damping effects on parametric decays of Alfvén waves, *J. Geophys. Res.*, *105*, 10,509.

Gomberoff, L., K. Gomberoff, and A. L. Brinca (2001), Ion acoustic damping effects on parametric decays of Alfvén waves: Right-hand polarization, *J. Geophys. Res.*, *106*, 18,713.

Hammett, G. W., and F. W. Perkins (1990), Fluid moment models for Landau damping with application to the ion-temperature-gradient instability, *Phys. Rev. Lett.*, *64*, 3019.

Hollweg, J. V. (1994), The beat, modulational and decay instabilities of a circularly polarized Alfvén wave, *J. Geophys. Res.*, *99*, 23,431.

Hollweg, J. V., R. Esser, and V. Jayanti (1993), Modulational and decay instability of Alfvén waves: Effects of streaming He++, *J. Geophys. Res.*, *98*, 3491.

Hoshino, M., and M. L. Goldstein (1989), Time evolution from linear to nonlinear stages in magnetohydrodynamic parametric instabilities, *Phys. Fluids B*, *1*, 1405.

Inhester, B. (1990), A drift-kinetic treatment of the parametric decay of large-amplitude Alfvén waves, *J. Geophys. Res.*, *95*, 10,525.

Lee, Y. C., and P. K. Kaw (1972), Parametric instabilities of ion cyclotron waves in a plasma, *Phys. Fluids*, *15*, 911.

Longtin, M., and B. U. Ö. Sonnerup (1986), Modulational instability of circularly polarized Alfvén waves, *J. Geophys. Res.*, *91*, 6816.

Marsch, E., and C.-Y. Tu (2001), Evidence for pitch-angle diffusion of solar wind protons in resonance with cyclotron waves, *J. Geophys. Res.*, *106*, 8359.

Medvedev, M. V., and P. H. Diamond (1996), Fluid models for kinetic effects on coherent nonlinear Alfvén waves. I. Fundamental theory, *Phys. Plasmas.*, *3*, 863.

Medvedev, M. V., P. H. Diamond, V. I. Shevchenko, and V. L. Galinsky (1997), Dissipative dynamics of collisionless nonlinear Alfvén wave trains, *Phys. Rev. Lett.*, *78*, 4934.

Minter, A. H., and S. R. Spangler (1997), Heating of the interstellar diffuse ionized gas via the dissipation of turbulence, *Astrophys. J.*, *485*, 182.

Mio, K., T. Ogino, K. Minami, and S. Takeda (1976), Modified nonlinear Schrödinger equation for Alfvén waves propagating along the magnetic field in cold plasmas, *Soc. Jpn.*, *41*, 265.

Mjølhus, E. (1976), On the modulational instability of hydromagnetic waves parallel to the magnetic field, *J. Plasma Phys.*, *16*, 321.

Mjølhus, E., and J. Wyller (1988), Nonlinear Alfvén waves in a finite-beta plasma, *J. Plasma Phys.*, *40*, 229.

Passot, T., and P.-L Sulem (2004), A Landau fluid model for dispersive magnetohydrodynamics, *Phys. Plasmas*, *11*, 5173.

Roberts, C. S., and S. J. Buchsbaum (1964), Motion of a charged particle in a constant magnetic field and a transverse electromagnetic wave propagating along the field, *Phys. Rev.*, *135*, A381.

Rogister, A. (1971), Parallel propagation of nonlinear low-frequency waves in high-β plasma, *Phys. Fluids*, *14*, 2733.

Ruderman, M. S., and D. Simpson (2004), The stability of parallel-propagating circularly polarized Alfvén waves revisited, *J. Plasma Phys.*, *70*, 143, doi:10.1017/S0022377803002599.

Spangler, S. R. (1989), Kinetic effects of Alfvén wave nonlinearity. I - Ponderomotive density fluctuations, *Phys. Fluids*, *B1*, 1738.

Spangler, S. R., and J. P. Sheerin (1982), Properties of Alfvén solitons in a finite-beta plasma, *J. Plasma Phys.*, *27*, 193.

Spangler, S. R., J. A. Leckband, and I. H. Cairns (1997), Observations of the parametric decay instability of nonlinear magnetohydrodynamic waves, *Phys. Plasmas*, *4*, 846.

Terasawa, T., M. Hoshino, J. Sakai, and T. Hada (1986), Decay instability of finite-amplitude circularly polarized Alfvén waves: A numerical simulation of stimulated Brillouin scattering, *J. Geophys. Res.*, *91*, 4171.

Tu, C-Y., and E. Marsch (1995), MHD structures, waves and turbulence in the solar wind: Observations and theories, *Space Sci. Rev.*, *73*, 1–210.

Tu, C.-Y., and E. Marsch (2001), On cyclotron wave heating and acceleration of solar wind ions in the outer corona, *J. Geophys. Res.*, *106*, 8233.

Vasquez, B. J. (1995), Simulation study of the role of ion kinetics in low-frequency wave train evolution, *J. Geophys. Res.*, *100*, 1779.

Viñas, A. F., and M. L. Goldstein (1991a), Parametric instabilities of circularly polarized large-amplitude dispersive Alfvén waves: Excitation of parallel-propagating electromagnetic daughter waves, *J. Plasma Phys.*, *46*, 107.

Viñas, A. F., and M. L. Goldstein (1991b), Parametric instabilities of circularly polarized large-amplitude dispersive Alfvén waves: Excitation of obliquely-propagating daughter and side-band waves, *J. Plasma Phys.*, *46*, 129.

Wang, C. B., C. S. Wu, and P. H. Yoon (2006), Heating of ions by Alfvén waves via nonresonant interactions, *Phys. Rev. Lett.*, *96*, 125,001.

Winske, D., and M. M. Leroy (1984), Diffuse ions produced by electromagnetic ion beam instabilities, *J. Geophys. Res.*, *89*, 2673.

Wong, H. K., and M. L. Goldstein (1986), Parametric instabilities of circularly polarized Alfvén waves including dispersion, *J. Geophys. Res.*, *91*, 5617.

J. A. Araneda, Departamento de Física, Facultad de Ciencias Fisicas y Matemáticas, Universidad de Concepción, Casilla 160-C, Concepción, Chile. (jaraneda@udec.cl)

E. Marsch, Max-Planck-Institut für Sonnensystemforschung, D-37191 Katlenburg-Lindau, Germany. (marsch@linmpi.mpg.de)

A. F. Viñas, Laboratory for Solar and Space Physics, Heliospheric Physics Branch, NASA Goddard Space Flight Center, Mail Code 612.2, Greenbelt, MD, 20771, USA. (adolfo.vinas@gsfc.nasa.gov)